2019 IEEE/RSJ International Conference on Intelligent Robots and Systems (IROS)
Macau, China, November 4-8, 2019

Model Simplification For Dynamic Control of Series-Parallel Hybrid Robots - A Representative Study on the Effects of Neglected Dynamics

Shivesh Kumar[1], Julius Martensen[3], Andreas Mueller[2] and Frank Kirchner[1,3]

***Abstract*— It is becoming increasingly popular to use parallel mechanisms as modular subsystem units in the design of various robots for their superior stiffness, payload-to-weight ratio and dynamic properties. This leads to series-parallel hybrid robotic systems which pose several challenges in their modeling and control e.g. resolution of loop closure constraints, large size of their spanning tree etc. These robots are typically position-controlled and when equipped with real time dynamic control, often a simplified inverse dynamic model of these systems is utilized. However, the trade-offs of this model simplification has not been studied previously. This paper presents a representative study of the neglected dynamics by introducing some error metrics which are useful in highlighting the advantages and disadvantages of such model simplification. The study is guided with the help of a series-parallel humanoid leg which has been recently developed at DFKI-RIC.**

I. INTRODUCTION

Serial and tree-type mechanisms are well known for their versatility in applications, large workspace, and simple modeling and control. Hence, they often represent the state-of-the-art in robotic systems. However, they generally feature only limited precision, low stiffness, and poor dynamic characteristics. For these reasons, legged robots based on a purely tree type topology suffer from speed and torque limitations. In contrast to serial robots, parallel devices can provide higher stiffness, speed, accuracy, and payload capacity. On the downside, they possess a reduced workspace and a more complex geometry which requires careful analysis and control. Parallel robots have been traditionally used in fast pick-and-place applications, driving simulators, fast orientation devices, rehabilitation to name a few applications. To combine the various advantages of serial and parallel topologies, many series-parallel hybrid designs, primarily in the field of legged robotics, have been developed in the last decade (see Fig. 1). Fig. 1a shows the bipedal robot LOLA [1] which is probably the first humanoid robot designed using a modular joint concept utilizing parallel kinematics. The design of NASA Valkyrie humanoid [2] followed a similar design concept by utilizing parallel kinematics for its wrist, torso and ankle joints. Fig. 1b shows the hominid robot CHARLIE [3], featuring a stewart platform of type 6-RUS as a six dof active joint in spine and neck. It also utilizes another parallel mechanism in the ankle joint. The multi-legged robot MANTIS [4] depicted in Fig. 1c contains parallel kinematic mechanisms (PKMs) of type 2-SPU+1U in its ankle joints and closed loop mechanisms of type 1-RRPR that drive certain revolute joints in its legs and torso. Fig. 1d demonstrates a highly modular light weight RECUPERA full-body exoskeleton [5], [6] with 32 active dofs which is built by combining several higher dof joint modules: a Stewart platform of type 6-UPS in torso, a double parallelogram [7] in shoulder for flexion–extension movement and ACTIVE ANKLE mechanism (type 3-R[2-SS]) [8] as a 3 dof joint in hip and ankle. Most of these hybrid robots utilize parallel submechanisms as an abstraction to a higher degree of freedom active joint (for e.g. universal, spherical, six dof). The design motivation of such hybrid robots is evident: use of PKM-based submechanisms helps designers to achieve light weight modular designs while enhancing the stiffness and dynamic characteristics of the robot. Moreover, a modular design saves manufacturing costs and integration time.

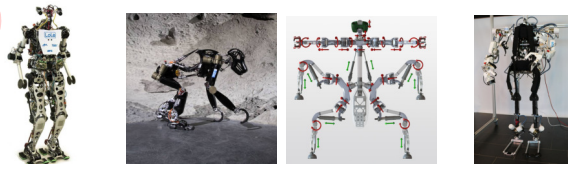

(a) Lola (b) Charlie (c) MANTIS (d) Recupera

Fig. 1: Examples of series-parallel Hybrid robots

The usage of parallel submechanisms in a robot's design introduces a new level of complexity to their description, kinematic and dynamic modeling and control. They are typically described with the help of topological graphs which are usually converted to spanning trees subjected to additional loop closure constraints [9], [10]. While loop closure constraints can be resolved for a general case using numerical techniques such as Baumgarte stabilisation, such solution methods are usually prone to inaccuracy and may suffer from poor computational performance. The Rigid Body Dynamics Library (`RBDL`) [11] and `OpenSim` [12] are some examples of open source libraries that implement generic algorithms for this purpose. Handcrafted analytical solutions to these constraints perform much better in terms of accuracy and computational performance but they come at a loss of generality. Recently, the authors have reported the development of a modular software workbench called, Hybrid Robot Dynamics (HyRoDyn) [13], which allows the resolution of the loop closure constraints in series-parallel hybrid systems

[1]Shivesh Kumar and Frank Kirchner are with the Robotics Innovation Center, German Research Center for Artificial Intelligence (DFKI GmbH), 28359 Bremen, Germany `shivesh.kumar@dfki.de`

[2]Andreas Mueller is with the Institute of Robotics, Johannes Kepler University, 4040 Linz, Austria `a.mueller@jku.at`

[3]Julius Martensen and Frank Kirchner are with the Department of Mathematics and Informatics, University of Bremen 28359 Bremen, Germany `julius.martensen@uni-bremen.de`, `frank.kirchner@dfki.de`

978-1-7281-4004-9/19/$31.00 ©2019 IEEE

HyRoDyn: series-parallel mechanism

analytically. Once, the loop closure constraints have been resolved, $O(n)$ algorithms for multi-body dynamics can be utilized to compute the solution to forward and inverse dynamics problems. Regardless of the way in which these constraints are resolved, the computational costs involved in the full kinematic and dynamic model is still relatively high in comparison to serial and tree type architectures due to large size of their spanning tree. Hence, these robots are often limited to position control (e.g. MANTIS, CHARLIE, SHERPATT) where a joint to actuator mapping is utilized to achieve a kinematic control of the robot.

Model order reduction vs Model simplification

Model order reduction (MOR) techniques aim to reduce the computational complexity of large scale mathematical models in computer simulations. Traditionally, this technique has been used for problems in fluid mechanics [14] and structural mechanics [15] to reduce the simulation time while making little compromises on the accuracy. As the complexity of rigid multi-body systems used in robotics is increasing, the need of MOR becomes indispensable for simulation and real-time control of modern contemporary robots. While this term is not classically used in the area of rigid body dynamics, the use of model simplification approach is common nevertheless. The moving parts inside a parallel submechanism module may have relatively small contribution to the overall dynamics of the system which is essentially due to dynamics of major link segments, and joint friction etc [16]. Hence, an inverse dynamic model in generalized coordinates is often combined with an inverse static model in actuation space to compute the actuator forces [17], [18], [19]. This approach is used in torque controlled series-parallel hybrid humanoids such as THOR, Valkyrie, Lola etc. The obvious advantage of this simplification is the reduced CPU time needed to solve the inverse dynamic model but it leads to unnecessary increase of PD gains for achieving the desired controller tracking performances.

Goals

To the best knowledge of the authors, the trade-off between the complete dynamic model and simplified dynamic model in the context of series-parallel hybrid robots has not been reported in the literature. The contribution of this paper is a study of the neglected dynamics in such a model simplification approach with the help of certain error metrics. An example of series-parallel hybrid humanoid leg is used in this study and its dynamics is excited in different ways. In particular, we study the effects of randomly drawn configurations from the state space of the serial model with zero acceleration and the effects of the model simplification given a target task space trajectory. The results from the study aims to provide insights into the advantages and disadvantages from the model simplification and to open new perspectives for research in model order reduction in rigid body dynamics.

Organization: Section 2 provides theoretical preliminaries for modeling robots with closed loops. It also discusses the nature of model simplification that has been adopted in the literature. Section 3 presents the error metrics adopted in the representative study. Section 4 presents the simulation scenarios and the results of this study with the help of a series-parallel hybrid humanoid leg. Section 5 draws the conclusions and presents future work.

II. MODELING AND CONTROL OF SERIES-PARALLEL HYBRID SYSTEMS

This section discusses the modeling and control of series-parallel hybrid robots. Further, we summarize the model simplification that is adopted for kinematic and dynamic control of these robots.

A. Loop Closure Constraints

Systems with closed loops are typically described with connectivity graphs ($\mathcal{G}$) where links and joints are denoted as vertices and edges respectively. A spanning tree ($\mathcal{T}$) is a subgraph of $\mathcal{G}$ such that there exists exactly one path between any two nodes in the graph and that the motion variables of $\mathcal{T}$ satisfy the loop closure constraints. Further, we identify three set of coordinates on ($\mathcal{G}$):

- spanning tree joints ($\boldsymbol{q} \in \mathbb{R}^n$): all the joints belonging to the spanning tree ($\mathcal{T}$) chosen by regular numbering scheme,
- independent joints ($\boldsymbol{y} \in \mathbb{R}^m$): the set of independent variables or generalized coordinates selected such that $\boldsymbol{y}$ defines $\boldsymbol{q}$ uniquely,
- active joints ($\boldsymbol{u} \in \mathbb{R}^p$): all the joints that contain the actuators

In the scope of this paper, we assume that the robot is fully actuated i.e. $p = m$. Loop constraints are algebraic constraints on the motion variables of a multi-body system. Loop constraints can be expressed in implicit explicit forms and have been summarized in Table I at position, velocity, and acceleration levels where ϕ and γ denote the position level loop constraints in implicit and explicit forms respectively. Here, $\boldsymbol{K} = \frac{\partial \phi}{\partial \boldsymbol{q}}$, $\boldsymbol{k} = -\dot{\boldsymbol{K}}\dot{\boldsymbol{q}}$, $\boldsymbol{G} = \frac{\partial \gamma}{\partial \boldsymbol{y}}$, and $\boldsymbol{g} = \dot{\boldsymbol{G}}\dot{\boldsymbol{y}}$. If both functions ϕ and γ describe the same constraint, $\phi \circ \gamma = \boldsymbol{0}$, $\boldsymbol{KG} = \boldsymbol{0}$, and $\boldsymbol{Kg} = \boldsymbol{k}$ can be deduced. Algorithms to compute variables in Table I from the spanning tree are provided in [9] and skipped here for brevity.

TABLE I: Loop constraints [9]

Type	position	velocity	acceleration
implicit:	$\phi(\boldsymbol{q}) = \boldsymbol{0}$	$\boldsymbol{K}\dot{\boldsymbol{q}} = \boldsymbol{0}$	$\boldsymbol{K}\ddot{\boldsymbol{q}} = \boldsymbol{k}$
explicit:	$\boldsymbol{q} = \gamma(\boldsymbol{y})$	$\dot{\boldsymbol{q}} = \boldsymbol{G}\dot{\boldsymbol{y}}$	$\ddot{\boldsymbol{q}} = \boldsymbol{G}\ddot{\boldsymbol{y}} + \boldsymbol{g}$

B. Equations of Motion (EOM)

The EOM for the spanning tree of a multi-body system with closed loops is given by

$$\boldsymbol{\tau} + \boldsymbol{\tau}_c = \boldsymbol{H}(\boldsymbol{q})\ddot{\boldsymbol{q}} + \boldsymbol{C}(\boldsymbol{q}, \dot{\boldsymbol{q}}) \tag{1}$$

where $\boldsymbol{q}, \dot{\boldsymbol{q}}, \ddot{\boldsymbol{q}}$ are $(n \times 1)$ vectors of joint position, velocity and acceleration variables of the spanning tree, $\boldsymbol{H}(\boldsymbol{q})$ is the $(n \times n)$ mass-inertia matrix, $\boldsymbol{C}(\boldsymbol{q}, \dot{\boldsymbol{q}})$ is a $(n \times 1)$ vector for Coriolis-centrifugal and gravity efforts, and $\boldsymbol{\tau}$ is the $(n \times 1)$ vector of force/torque variables. Further, $\boldsymbol{\tau}_c$ is the unknown

vector of constraint forces produced by the cut joints but it can be eliminated from the equation following the Jourdain's principle of virtual power, i.e., $\boldsymbol{\tau}_c \dot{\boldsymbol{q}} = 0$. Using velocity level loop closure constraint and Jourdain's principle of virtual power, one can establish that $\boldsymbol{\tau}_c$ will have the following property

$$\boldsymbol{G}^T \boldsymbol{\tau}_c = 0\,. \tag{2}$$

By using Equation 2 and multiplying by $\boldsymbol{G}^T$ on both sides of Equation 1, the loop constraint forces $\boldsymbol{\tau}_c$ can be eliminated.

$$\boldsymbol{G}^T \boldsymbol{\tau} = \boldsymbol{G}^T (\boldsymbol{H}\ddot{\boldsymbol{q}} + \boldsymbol{C}) = \boldsymbol{G}^T \boldsymbol{\tau}_q \tag{3}$$

where $\boldsymbol{\tau}_q$ is the inverse dynamics output of the spanning tree given by $\boldsymbol{\tau}_q = \boldsymbol{H}(\gamma(\boldsymbol{y}))(\boldsymbol{G}\ddot{\boldsymbol{y}} + \boldsymbol{g}) + \boldsymbol{C}(\gamma(\boldsymbol{y}), \boldsymbol{G}\dot{\boldsymbol{y}})$. To arrive at a unique solution of Equation 3, the actuated DOF must be separated from the passive DOF. This can be done with the help of a $(m \times m)$ actuator Jacobian matrix $\boldsymbol{G}_u$ which basically contains the rows of $\boldsymbol{G}$ corresponding to the actuated DOF. Thus, the unique solution to the inverse dynamics (ID) problem is given by:

$$\boldsymbol{\tau}_u = \boldsymbol{G}_u^{-T} \boldsymbol{G}^T \boldsymbol{\tau}_q \tag{4}$$

where $\boldsymbol{\tau}_u$ is a $(m \times 1)$ vector of actuator forces required to produce the given acceleration $\ddot{\boldsymbol{y}}$.

C. Exploiting Modularity in Design

As noted previously in the Introduction, series-parallel hybrid robots often employ parallel mechanisms as an abstraction to various kinematic joint types (e.g. revolute, universal, spherical etc.). This modularity can be exploited in the resolution of loop closure constraints. In particular, this reveals a block diagonal structure in the loop closure Jacobian formulation (Fig. 2). This block diagonal structure is advantageous in solving Equation 4, for example. Further, the loop closure constraints of each submechanism module can be resolved locally. This idea forms the basis of a modular software workbench called HyRoDyn [13], [20] which provides closed form solutions to various parallel submechanism modules of different types and enables the analytical computation of kinematics and dynamics of arbitrary series-parallel hybrid robots composed of these modules. This tool is ideal for the model simplification studies as it enables very flexible composition of series-parallel hybrid models with variable fidelities.

D. Model Simplification and Control

Series-parallel hybrid robots are highly complex mechatronic systems and generic treatment of such robots remains an open problem. However, modularity in robot design allows for certain abstractions which simplifies their modeling and control. Such abstractions are shown in Fig. 3. While Fig. 3(a) captures the true complexity of the robot, due to absence of generic methods to model and control such systems, three different abstractions are adopted to simplify the modeling and control. In the following, we discuss the practices used in kinematic and dynamic control of series-parallel hybrid robots.

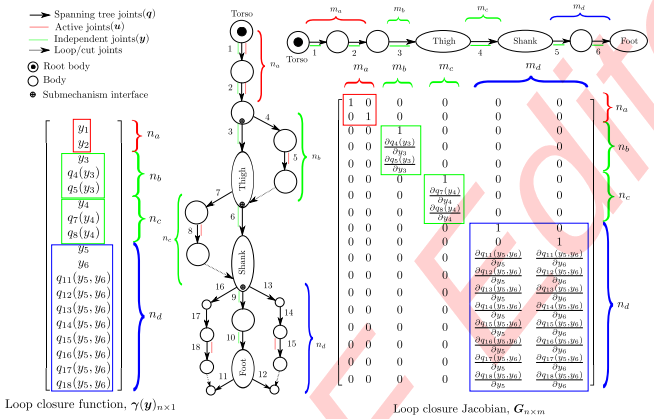

Fig. 2: Block diagonal structure in loop closure Jacobian

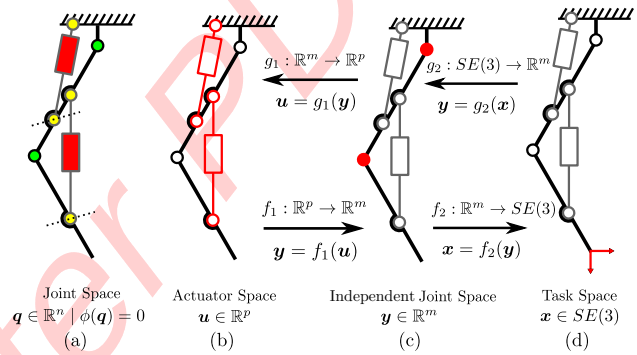

Fig. 3: Abstraction in series-parallel hybrid robots

a) Kinematics: Unlike serial designs, both forward and inverse kinematics problems for parallel mechanisms may have multiple solutions. It is common practice to avoid any switch of assembly and working modes in the design of parallel submechanism modules for hybrid robots. It is achieved by choosing appropriate design parameters and physically restricting the movement of the joints in the parallel submechanism module. Forward and inverse kinematics of the submechanism module is usually solved to provide a bi-directional map between actuation space and independent joint space (see Fig. 3(b) & (c)). They can be solved either analytically on local controllers or in resource-constrained systems with the help of Look Up Tables (LUTs). Once a mapping is available, the robot can be treated purely as a serial or tree type structure for which forward and inverse kinematics problems are easier to solve (see Fig. 3(d)). Many series-parallel hybrid robots such as SherpaTT [21], MANTIS and Charlie are kinematically controlled and compliance is realized only with the help of force/torque measurements. Further, it is not common practice to compute the full kinematic state of the spanning tree (see Fig. 3(a)) since such calculations can be computationally expensive.

b) Dynamics: As pointed out before, the computation of full inverse dynamic model for hybrid robots can be computationally expensive due to the large size of their spanning trees and the large number of loop closure constraints to

be resolved. For example, RH5 humanoid [22] which only contains relatively simple parallel mechanism modules (with less than 3 DOF) has 32 DOF ($m = p = 32$), $c = 15$ independent closed loops and $n = 76$ DOF in its spanning tree. The moving parts inside a parallel submechanism module may have relatively small contribution to the overall dynamics of the system which is essentially due to dynamics of major link segments lying on the trunk of the spanning tree and joint friction etc [16]. Hence, they may be left unmodeled or their mass-inertia properties can be merged to the larger link segments which are relevant to the independent joint space of the robot. Assuming actuators are the ideal torque source in the system, a simplified inverse dynamic model (see Fig. 3(c)) in independent joint space is often combined with an inverse static model in actuation space (see Fig. 3(b)) to compute the actuator forces [17], [18] using

$$\boldsymbol{\tau}_u = \boldsymbol{G}_u^{-T} \boldsymbol{\tau}_y \tag{5}$$

This approach is used in model based torque controlled series-parallel hybrid humanoids such as THOR, Valkyrie, Lola etc.

III. ERROR AND PERFORMANCE METRICS

The following section presents the implicit and explicit metrics used to describe and quantify the model simplification error. To be as physically meaningfull as possible, most of the described metrics are given in terms of the structural components of the EOM or as physical quantities, namely actuator forces, inertia tensor, energy and power. To some extent, statistical measurements have been used to qualitatively describe the relation of variables of the system with the resulting physical measurements. Explicit metrics can be directly measured or derived from the given data. Implicit metrics are rather of theoretical nature and serve the purpose of understanding the effects of the model simplification. To fullfill the definition of a metric, the 1-norm and 2-norm are used. Quantities related to the simplified model are expressed with upper hat notation.

A. Computation Time

A first metric is given by the raw computation time of the inverse dynamics problem, $t_{ID} \in \mathbb{R}^+$. It is an explicit metric and relates to the computational effort of the algorithm. All computations have been performed on a standard laptop with Intel Core i7 CPU @ 2.8 GHz using HyRoDyn software tool.

B. Generalized Inertia Tensor Error

The inertia tensor of a rigid body system plays an important role in the EOM, influencing the systems dynamics both directly via the acceleration and indirectly via the corriolis forces. Due to the simplification, inertias are either neglected or assumed to be static, hence introducing a configuration dependent error on the dynamics. The error is implicitly involved in the divergence of the models and serves as a base for discussion rather than a direct indicator. The error of the generalized inertia tensor $\Delta \boldsymbol{H}(\boldsymbol{y}) \in \mathbb{R}^{m \times m}$ is given by

$$\Delta \boldsymbol{H}(\boldsymbol{y}) = \boldsymbol{H}(\boldsymbol{y}) - \hat{\boldsymbol{H}}(\boldsymbol{y}) \tag{6}$$

With a metric defined by the induced 2-norm on $\Delta \boldsymbol{H}(\boldsymbol{y})$

$$\|\Delta \boldsymbol{H}(\boldsymbol{y})\|_2 = \sigma_{max}\left(\Delta \boldsymbol{H}(\boldsymbol{y})\right) \tag{7}$$

where $\sigma \in \mathbb{R}^+$ denotes the singular values of the matrix, which are equal to the eigenvalues iff the matrix is symmetric and positive-definite. This is the case for generalized mass-inertia matrix.

C. Actuator Force Error

Since the actuator forces given by the inverse dynamic model of a system are used as an input to the low-level PD controller, the resulting error $\Delta \boldsymbol{\tau}_u \in \mathbb{R}^p$ between $\mathcal{T}$ and $\hat{\mathcal{T}}$ is given by

$$\begin{aligned} \Delta \boldsymbol{\tau}_u &= \boldsymbol{\tau}_u - \hat{\boldsymbol{\tau}}_u && (8) \\ &= \left(\boldsymbol{H}(\boldsymbol{u}) - \hat{\boldsymbol{H}}(\boldsymbol{u})\right)\ddot{\boldsymbol{u}} + \boldsymbol{C}(\boldsymbol{u}, \dot{\boldsymbol{u}}) - \hat{\boldsymbol{C}}(\boldsymbol{u}, \dot{\boldsymbol{u}}) \\ &= \Delta \boldsymbol{H}(\boldsymbol{u})\ddot{\boldsymbol{u}} - \Delta \boldsymbol{C}(\boldsymbol{u}, \dot{\boldsymbol{u}}) && (9) \end{aligned}$$

is used as an explicit metric to measure the stiffness of the controllers. It denotes the individual differences of the actuation forces between the full and simplified models. Combining 5 and 3 gives the following expression for the torque error

$$\begin{aligned} \|\Delta \boldsymbol{\tau}_u\|_2 &= \left\| \boldsymbol{G}_u^{-T} \left(\boldsymbol{G}^T - \begin{bmatrix} \boldsymbol{I} & \boldsymbol{0} \end{bmatrix} \right) \boldsymbol{\tau}_q \right\|_2 \\ &\leq \|\Delta \boldsymbol{G}(\boldsymbol{q})\|_2 \left\| \boldsymbol{\tau}_q \right\|_2 \end{aligned} \tag{10}$$

where $\boldsymbol{\tau}_q$ is mapped onto the independent joints via the matrix $\begin{bmatrix} \boldsymbol{I} & \boldsymbol{0} \end{bmatrix}$. The 2-norm of the torque error is bounded from below and above via the singular values of the transformation define by $\Delta \boldsymbol{G} \in \mathbb{R}^{p \times n}$

$$\sigma_{min}\left(\Delta \boldsymbol{G}(\boldsymbol{q})\right) \leq \|\Delta \boldsymbol{\tau}_{\boldsymbol{u}}\|_2 \leq \sigma_{max}\left(\Delta \boldsymbol{G}(\boldsymbol{q})\right) \tag{11}$$

D. Energy Error

The evolution of the system is constrained via its total energy $E \in \mathbb{R}^+$ given by the following equivalent notations

$$\begin{aligned} E = K + U &= \frac{1}{2}\dot{\boldsymbol{q}}^T \boldsymbol{H}(\boldsymbol{q})\dot{\boldsymbol{q}} + U(\boldsymbol{q}) && (12) \\ &= \frac{1}{2}\dot{\boldsymbol{u}}^T \boldsymbol{H}(\boldsymbol{u})\dot{\boldsymbol{u}} + U(\boldsymbol{u}) \\ &= \frac{1}{2}\dot{\boldsymbol{y}}^T \boldsymbol{H}(\boldsymbol{y})\dot{\boldsymbol{y}} + U(\boldsymbol{y}) \end{aligned}$$

Equation (12) shows that the total energy can be defined via the coordinates associated with spanning tree, independent or active joints and their velocities. Here $K \in \mathbb{R}^+$ denotes the kinetic and $U \in \mathbb{R}^+$ the potential energy. Since, we assume the states to be equivalent, the only difference in energy can originate from either an error of the inertia matrix or an error in potential energy. We define the corresponding metric as the absolute value of the difference of the total energy $\Delta E \in \mathbb{R}^+$

$$\begin{aligned} \Delta E &= \left\| \frac{1}{2}\dot{\boldsymbol{y}}^T \left(\boldsymbol{H}(\boldsymbol{y}) - \hat{\boldsymbol{H}}(\boldsymbol{y}) \right) \dot{\boldsymbol{y}} + U(\boldsymbol{y}) - \hat{U}(\boldsymbol{y}) \right\|_1 && (13) \\ &= \left\| \frac{1}{2}\dot{\boldsymbol{y}}^T \Delta \boldsymbol{H}(\boldsymbol{y})\dot{\boldsymbol{y}} + \Delta U(\boldsymbol{y}) \right\|_1 \end{aligned}$$

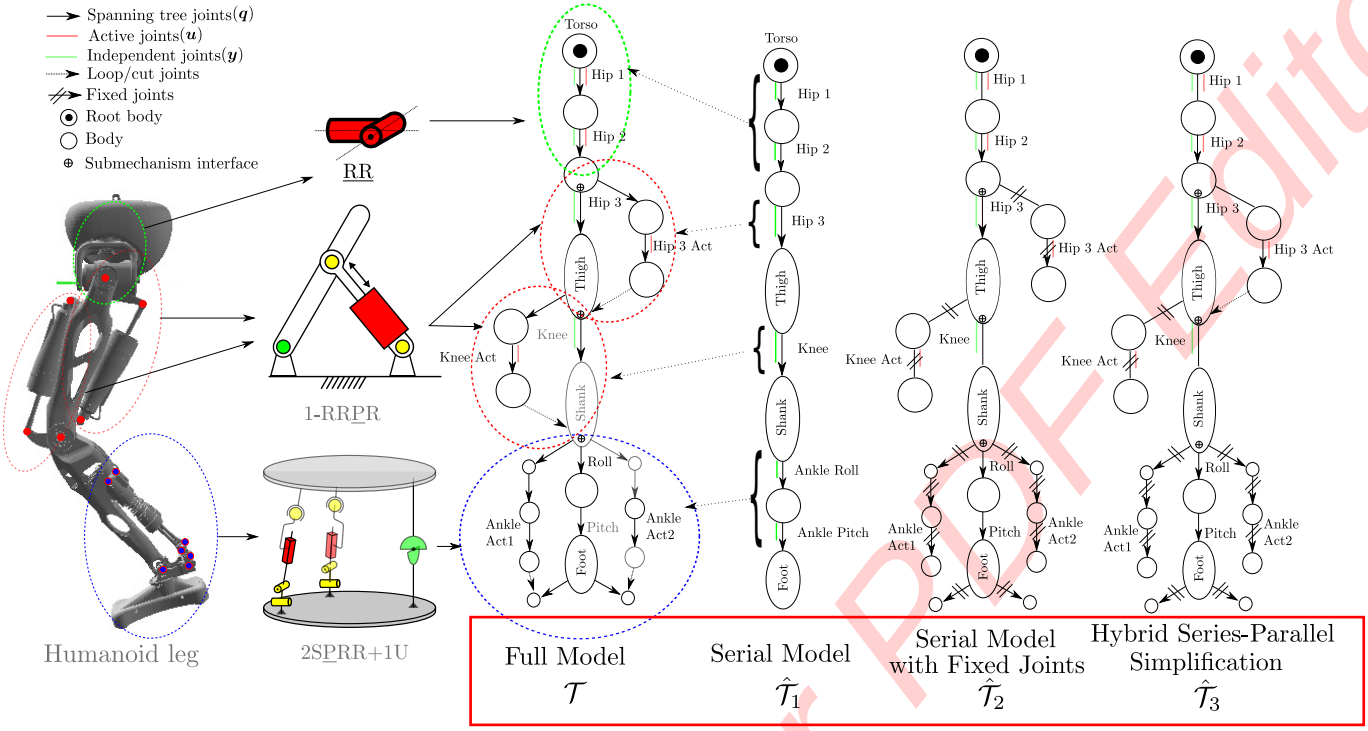

Fig. 4: Serial-Parallel hybrid composition of the RH5 leg and assumed simplifications

E. *Power Error Metric*

Like energy, the power $P \in \mathbb{R}$ associated to a system is an important explicitly measureable metric. The power, given by Jourdain's Principle, is invariant to coordinate transformation and can therefore be used to describe the input-output behaviour of a system.

$$P = \boldsymbol{\tau}_q^T \dot{\boldsymbol{q}} = \boldsymbol{\tau}_u^T \dot{\boldsymbol{u}} = \boldsymbol{\tau}_y^T \dot{\boldsymbol{y}} \tag{14}$$

The total power error can be expressed as a sum of power error of each individual submechanism $i \in \{1, \ldots, s\}$.

$$\Delta P = \left\| \sum_{i=1}^{s} \Delta \boldsymbol{\tau}_{ui}^T \dot{\boldsymbol{u}}_i \right\|_1 \tag{15}$$

IV. SIMPLIFICATION STUDIES AND RESULTS

The subject of interest within this study is the leg of the RH5 humanoid [22], currently being developed at the DFKI-RIC. Fig. 4 shows the serial-parallel hybrid mechanism consisting of 4 individual submechanism of types RR, 1-RRPR and 2SPRR+1U [23]. The full model of the leg ($\mathcal{T}$) has $m = 6$ independent degrees of freedom, $p = 6$ active joints and $n = 18$ spanning tree joints. Further, we introduce three different model simplifications from the full description of the robot: 1) $\hat{\mathcal{T}}_1$ is a subgraph of $\mathcal{T}$ containing only the independent joints neglecting all other branches, 2) $\hat{\mathcal{T}}_2$ is a subgraph of $\mathcal{T}$ containing only the independent joints where bodies separated by the cut joints in $\mathcal{T}$ are merged to parent and child links of each parallel submechanism module with the help of fixed joints [1], 3) $\hat{\mathcal{T}}_3$ is a subgraph of $\mathcal{T}$ which includes the Hip3 submechanism but the rest of the kinematic chain is kept serial like $\hat{\mathcal{T}}_2$. For the simplified models, it is assumed that actuators are still the ideal sources of forces or power. Further, the bi-directional kinematic mapping between the independent joint space and the actuator space is preserved. In the following, we present a Monte Carlo study in the generalized coordinates and a task space trajectory input to the models to study the effect of neglected dynamics. All the simulations are performed using HyRoDyn [13], [20].

[1]It should be noted that the total mass of $\hat{\mathcal{T}}_1$ is less than $\mathcal{T}$ and $\hat{\mathcal{T}}_2$ and $\mathcal{T}$ have equal masses.

A. *Monte Carlo Experiments*

In this study, random states drawn out of a uniform distribution over the generalized position limits of the hardware and small velocity limits between $[-0.1, +0.1]$ rad/s are assigned to the independent joints. Each joint has zero acceleration, which simplifies (4) to $\boldsymbol{\tau}_u = \boldsymbol{G}_u^{-T} \boldsymbol{G}^T \boldsymbol{C}(\boldsymbol{y}, \dot{\boldsymbol{y}})$. Further, either all the joints or individual joints in the model are assigned a selected position and velocity. For each study, 10000 samples were drawn and dynamic behavior of $\mathcal{T}$ and $\hat{\mathcal{T}}_2$ is compared as the two models have equivalent mass-inertia properties in the zero configuration.

In Fig. 5 the absolute error of the actuator forces is shown over the active joint state $(u, \dot{u})$. The comparison of all sampled independent joint states shows that depending on the configuration of the mechanism, model simplification may lead to large errors due to wrongly estimated Coriolis forces. While Ankle Act 1, Ankle Act 2 and Hip 1 show no obvious pattern in the error, the error in Hip 3 Act and Hip 2 seem to be influenced by the current position of the corresponding actuator. Hip 3 Act exhibits an increasing

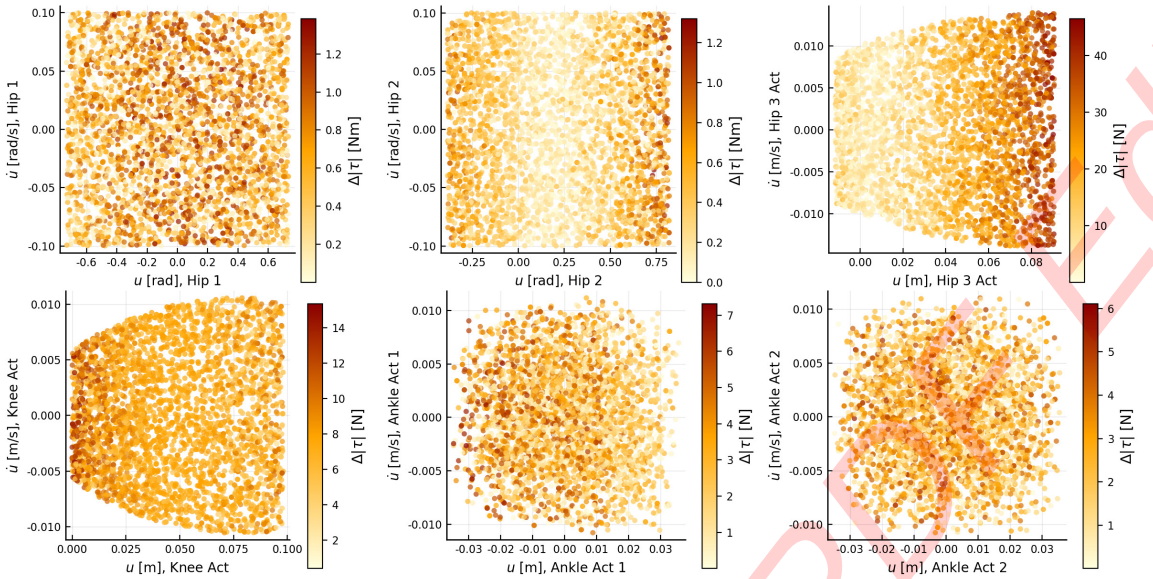

Fig. 5: State dependent error of the actuator forces in the Monte Carlo studies

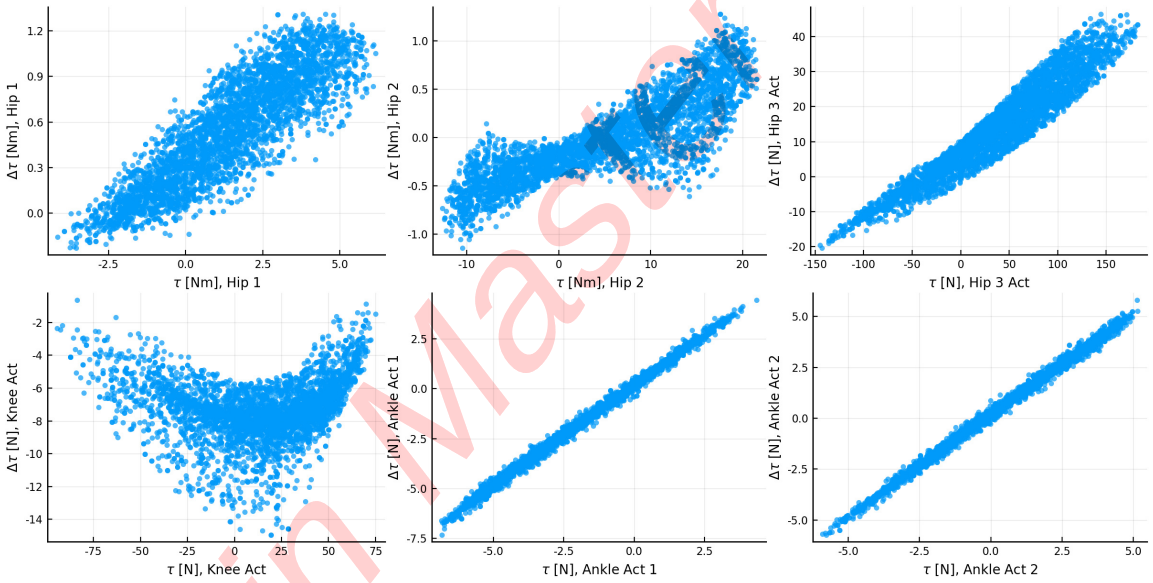

Fig. 6: Error of the actuator forces between full and simplified models in the Monte Carlo studies

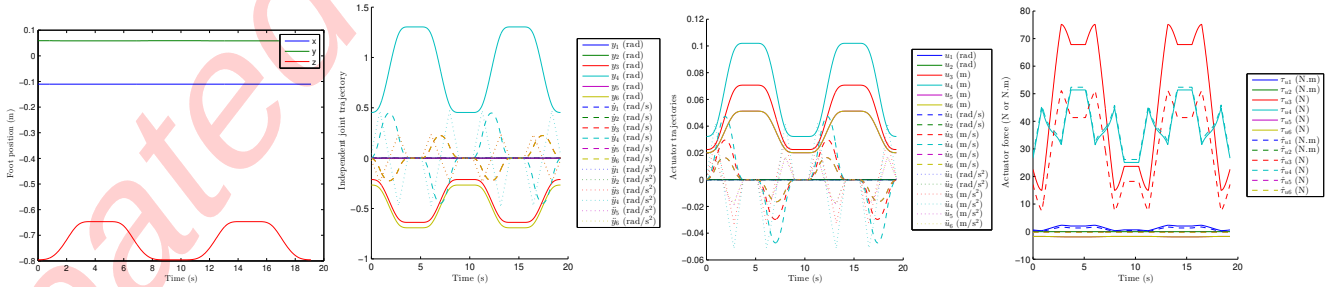

(a) Foot position (b) Independent joint trajectories (c) Actuator trajectories (d) Actuator forces comparison

Fig. 7: Task space and independent joint space trajectories of RH5 leg for up-down movement

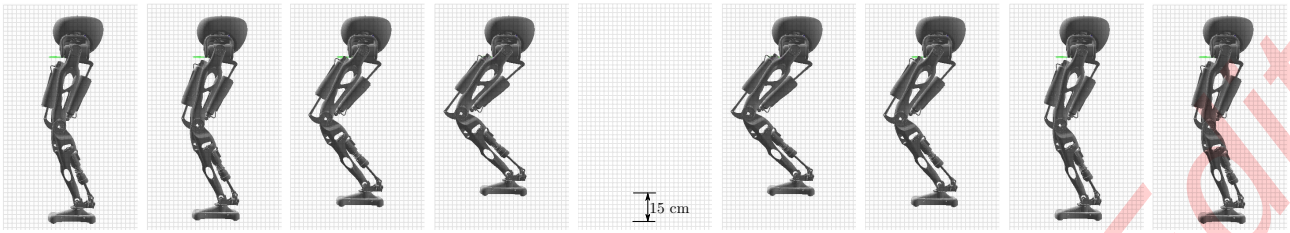

Fig. 8: Animation of up-down movement with RH5 leg

error with the position of the joint, reaching its maximum value near the upper limit of its motion range. The difference in force regarding Knee Act seems to be rather constant in its magnitude over the state space except at its limits.
The relationship between the actuator force error and the actual actuator force is shown in Fig. 6. The plots can be roughly interpreted as low dimensional cuts of the high dimensional space in which the system evolves. The error resulting from the Hip 2 and Knee Act is small in contrast to the actual forces of the actuator, while the error margin of Ankle, Hip 1 and Hip 3 actuators is varying between 25 and 100 %. Since Ankle Act 1 and Ankle Act 2 form a nearly straight line, a linear relationship between the error and actuator force can be suspected. Additionally, these plots show a qualitatively similar shape but do not incorporate the symmetry given by the submechanism structure. This is related to the absence of closed loop constraints, which would redistribute the forces throughout the mechanism. While Hip 3 Act seems to incorporate a similar relationship between the actuator force of the full and simplified model, other influences seem to take an effect on the error, since its lower dimensional representation forms a surface. Hip 1, Hip 2, Hip 3 Act and Knee Act show a strong relationship to other influences. The actuator force error range is smaller for the submechanisms that are farther away from the root link because it is common design practice to have smaller distal masses.

In Fig. 9, the accumulated power which is the sum of power of each submechanism given by (14) over all samples in the state space is shown. Fig. 9a shows the results of the study with fully randomized excitation of $\boldsymbol{y}$ and $\dot{\boldsymbol{y}}$. The largest error is located in the submechanism corresponding to Hip 3. In Fig. 9b, a similar observation for Hip 3 can be made for individual excitation, while the error related to the Knee submechanism is very small.

B. Workspace Trajectory

We present a comparison between the full model ($\mathcal{T}$) and simplified models ($\hat{\mathcal{T}}_i, i \in \{1,2,3\}$) in task space control of the humanoid leg. Two set points i.e. foot up position & foot down position, separated by 15 cm in z-direction, are chosen in the task space of the robot. Using the inverse kinematics, the independent joint positions are computed which can be done either numerically or analytically. Then, these way-points in independent joint space are fed to an interpolator which provides smooth trajectories $(\boldsymbol{y}, \dot{\boldsymbol{y}}, \ddot{\boldsymbol{y}})$ for

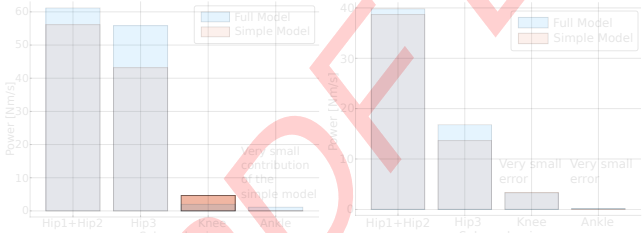

(a) Full Excitation (b) Individual Excitation

Fig. 9: Accumulated power of the individual submechanism in the Monte Carlo studies

up and down movement of the leg. Fig. 7a and Fig. 7b shows the task space and independent joint space trajectories for the RH5 leg. These trajectories are then used to compute the actuator trajectories $(\boldsymbol{u}, \dot{\boldsymbol{u}}, \ddot{\boldsymbol{u}}, \boldsymbol{\tau}_u)$ using inverse kinematics and inverse dynamics algorithms as presented earlier. Fig. 7c shows the position, velocity, acceleration required in different actuators of the robot to produce this movement for both the models as they share the same inverse kinematics mapping. However, full spanning tree state $(\boldsymbol{q}, \dot{\boldsymbol{q}}, \ddot{\boldsymbol{q}})$ is computed for $\mathcal{T}$ which can be used for robot visualization (see Fig. 8). The effect of neglected dynamics due to model simplification can be observed in Fig. 7d which compares the acuator forces between the two models ($\mathcal{T}$ & $\hat{\mathcal{T}}_2$). As expected from the Monte Carlo study, the highest error is in Hip 3 Act joint.

C. Discussion

The results of the Monte Carlo study show that certain submechanism modules are more prone to contributing to the overall error than others during the model simplification. In general, it was observed that $\hat{\mathcal{T}}_1$ performs worse than $\hat{\mathcal{T}}_2$ due to the missing masses and the results have been skipped here for brevity. The branches in Hip 3 and Knee submechanisms have relatively higher masses and inertias than the branches in the Ankle submechanism and hence are more prone to influencing the error in overall dynamics of the system. The comparison of average CPU time for solving inverse dynamics (per call) and relative error in power between the full and simplified models is shown in Table II for the workspace trajectory following study. It can be noticed that model simplifications definitely provide a computational advantage in solving inverse dynamics for real time control. In the state of the art, it has been considered as a rule of thumb that a simplified model neglecting all the closed loops is sufficient for dynamic control. However, this is not true as

Common Practice

TABLE II: Comparison of CPU time and relative power error between the full and simplified models

	Model (n)	Rel. Power Error ($\frac{\Delta P}{P}$ %)	t_{ID} (µs)	Speedup w.r.t. $\mathcal{T}$ ($\frac{t_{ID}-\hat{t}_{ID}}{t_{ID}}$ %)
full	$\mathcal{T}$ (18)	-	32.03	-
serial	$\hat{\mathcal{T}}_1$ (6)	53.24	12.08	62.28
	$\hat{\mathcal{T}}_2$ (6)	12.43	12.08	62.28
serial + 1 parallel	$\hat{\mathcal{T}}_3$ (8)	3.05	14.32	55.41

Central Outcome

certain closed loops may affect the error dynamics more than others and simplified models respecting those loop closure constraints outperform these models in terms of accuracy without compromising much on the CPU time. For example, the simplified model $\hat{\mathcal{T}}_3$ which respects the loop closure constraints in Hip3 submechanism (see Fig. 4) adds only 2 extra DOF to the spanning tree in comparison to $\hat{\mathcal{T}}_2$ brings down the relative power error to ≈ 3 % while taking only $\approx 2\mu$s extra in computation of inverse dynamics.

V. CONCLUSION AND OUTLOOK

This paper presents a study of neglected dynamics during model simplification in series-parallel hybrid robots. As the complexity of robotic systems and the need of their fast dynamic control is increasing, model simplification in rigid body dynamics is becoming important. To find a reduced order model which decreases the computational effort without compromising much on the accuracy is an interesting problem. This could also provide some insights on how to select the appropriate set of cut joints and generalized coordinates to properly describe the system. It is clear that reduced models of high fidelity are strongly linked with the state space and hence it is also interesting to study a family of reduced (order) models for different contexts and controllers that allow smooth transitions between them.

ACKNOWLEDGMENT

This work was performed performed within the Q-RoCK project, funded by the German Aerospace Center (DLR) with federal funds from the Federal Ministry of Education and Research (BMBF) (Grant Number: FKZ 01IW18003). The third author acknowledges the support from the LCM K2 Center for Symbiotic Mechatronics within the framework of the Austrian COMET-K2 program.

REFERENCES

[1] S. Lohmeier, T. Buschmann, H. Ulbrich, and F. Pfeiffer, "Modular joint design for performance enhanced humanoid robot lola," in *Proceedings 2006 IEEE International Conference on Robotics and Automation, 2006. ICRA 2006.*, May 2006, pp. 88–93.

[2] N. A. Radford and et. al., "Valkyrie: Nasa's first bipedal humanoid robot," *Journal of Field Robotics*, vol. 32, no. 3, pp. 397–419, 2015. [Online]. Available: http://dx.doi.org/10.1002/rob.21560

[3] D. Kuehn, F. Bernhard, A. Burchardt, M. Schilling, T. Stark, M. Zenzes, and F. Kirchner, "Distributed computation in a quadrupedal robotic system," *International Journal of Advanced Robotic Systems*, vol. 11, no. 7, p. 110, 2014.

[4] S. Bartsch, M. Manz, P. Kampmann, A. Dettmann, H. Hanff, M. Langosz, K. v. Szadkowski, J. Hilljegerdes, M. Simnofske, P. Kloss, M. Meder, and F. Kirchner, "Development and control of the multi-legged robot mantis," in *Proceedings of ISR 2016: 47st International Symposium on Robotics*, June 2016, pp. 1–8.

[5] E. A. Kirchner, N. Will, M. Simnofske, L. M. V. Benitez, B. Bongardt, M. M. Krell, S. Kumar, M. Mallwitz, A. Seeland, M. Tabie, H. Whrle, M. Yksel, A. He, R. Buschfort, and F. Kirchner, "Recupera-reha: Exoskeleton technology with integrated biosignal analysis for sensorimotor rehabilitation," in *Transdisziplinre Konferenz SmartASSIST*, 2016, pp. 504–517.

[6] S. Kumar and et. al., "Modular design and decentralized control of the recupera exoskeleton for stroke rehabilitation," *Applied Sciences*, vol. 9, no. 4, 2019. [Online]. Available: http://www.mdpi.com/2076-3417/9/4/626

[7] S. Kumar, M. Simnofske, B. Bongardt, A. Mueller, and F. Kirchner, "Integrating mimic joints into dynamics algorithms exemplified by the hybrid recupera exoskeleton," in *Advances In Robotics (AIR-2017), June 28 - July 2, New Delhi, India*. ACM-ICPS, 2017.

[8] S. Kumar, B. Bongardt, M. Simnofske, and F. Kirchner, "Design and kinematic analysis of the novel almost spherical parallel mechanism active ankle," *Journal of Intelligent & Robotic Systems*, Mar 2018. [Online]. Available: https://doi.org/10.1007/s10846-018-0792-x

[9] R. Featherstone, *Rigid Body Dynamics Algorithm*, 2008.

[10] A. Jain, *Robot and Multibody Dynamics: Analysis and Algorithms*. Springer Verlag, 2011.

[11] M. L. Felis, "Rbdl: an efficient rigid-body dynamics library using recursive algorithms," *Autonomous Robots*, vol. 41, no. 2, pp. 495–511, 2017.

[12] S. L. Delp, F. C. Anderson, A. S. Arnold, P. Loan, A. Habib, C. T. John, E. Guendelman, and D. G. Thelen, "Opensim: Open-source software to create and analyze dynamic simulations of movement," *IEEE Transactions on Biomedical Engineering*, vol. 54, no. 11, pp. 1940–1950, Nov 2007.

[13] S. Kumar, K. A. von Szadkowski, A. Mller, and F. Kirchner, "HyRoDyn: A modular software framework for solving analytical kinematics and dynamics of series-parallel hybrid robots," in *International Conference on Intelligent Robots and Systems*, ser. IROS Poster, Oct. 2018.

[14] T. Lassila, A. Manzoni, A. Quarteroni, and G. Rozza, *Model Order Reduction in Fluid Dynamics: Challenges and Perspectives*. Cham: Springer International Publishing, 2014, pp. 235–273. [Online]. Available: https://doi.org/10.1007/978-3-319-02090-7_9

[15] L. Wu and P. Tiso, "Nonlinear model order reduction for flexible multibody dynamics: a modal derivatives approach," *Multibody System Dynamics*, vol. 36, no. 4, pp. 405–425, Apr 2016. [Online]. Available: https://doi.org/10.1007/s11044-015-9476-5

[16] T. Buschmann, V. Favot, M. Schwienbacher, A. Ewald, and H. Ulbrich, "Dynamics and control of the biped robot lola," in *Multibody System Dynamics, Robotics and Control*, H. Gattringer and J. Gerstmayr, Eds. Vienna: Springer Vienna, 2013, pp. 161–173.

[17] M. A. Hopkins, S. A. Ressler, D. F. Lahr, A. Leonessa, and D. W. Hong, "Embedded joint-space control of a series elastic humanoid," in *2015 IEEE/RSJ International Conference on Intelligent Robots and Systems (IROS)*, Sept 2015, pp. 3358–3365.

[18] P. Vonwirth, "Modular control architecture for bipedal walking on a single compliant leg," Master's Thesis, Robotics Research Lab, University of Kaiserslautern, September 2017, unpublished; supervised by Steffen Schütz.

[19] N. Paine, J. S. Mehling, J. Holley, N. A. Radford, G. Johnson, C.-L. Fok, and L. Sentis, "Actuator control for the nasa-jsc valkyrie humanoid robot: A decoupled dynamics approach for torque control of series elastic robots," *Journal of Field Robotics*, vol. 32, no. 3, pp. 378–396. [Online]. Available: https://onlinelibrary.wiley.com/doi/abs/10.1002/rob.21556

[20] S. Kumar and A. Mueller, "An analytical and modular software workbench for solving kinematics and dynamics of series parallel hybrid robots," in *ASME 2019 International Design Engineering Technical Conferences and Computers and Information in Engineering Conference*, ser. 43rd Mechanisms and Robotics Conference.

[21] F. Cordes, A. Babu, and F. Kirchner, "Static force distribution and orientation control for a rover with an actively articulated suspension system," in *2017 IEEE/RSJ International Conference on Intelligent Robots and Systems (IROS)*, Sept 2017, pp. 5219–5224.

[22] H. Peters, P. Kampmann, and M. Simnofske, "Konstruktion eines zweibeinigen humanoiden roboters," in *2. VDI Fachkonferenz Humanoide Roboter*, Dec 2017.

[23] S. Kumar, A. Nayak, H. Peters, C. Schulz, A. Mueller, and F. Kirchner, "Kinematic analysis of a novel parallel 2sprr+1u ankle mechanism in humanoid robot," in *Advances in Robot Kinematics*, M. Carricato, Ed. Cham: Springer Verlag GmbH, 2018.